Precious Metal−Molecular Oxygen Complexes: Neon Matrix Infrared Spectra and Density Functional Calculations for $M(O_2)$, $M(O_2)_2$ (M = Pd, Pt, Ag, Au)

Xuefeng Wang and Lester Andrews*

Department of Chemistry, University of Virginia, McCormick Road, P.O. Box 400319, Charlottesville, Virginia 22904-4319

Received: January 7, 2001; In Final Form: March 29, 2001

Laser-ablated palladium, platinum, silver, and gold atoms react with molecular oxygen in excess neon during condensation at 4 K. Reaction products, M-(η^2-OO), M-(η^2-OO)$_2$ (M = Pd, Pt), PtO, PtO_2, AuO_2, M-(η^1-OO) (M = Ag, Au), and anions Ag-(η^1-OO)$^-$, Au-(η^1-OO)$_2^-$, are identified from isotopic shifts and splittings in their matrix infrared spectra. Density functional theory (BPW91 and B3LYP) calculations are performed on the product molecules for comparison of calculated frequencies and $^{16}O/^{18}O$ isotopic ratios. Doping with CCl_4 to serve as an electron trap eliminates the anion bands, which further supports the anion identifications. The reaction mechanism and comparison with argon matrix experiments are discussed. The AuOO complex exhibits an unusually large neon−argon matrix shift, which suggests increased charge transfer in the more polarizable argon matrix.

Introduction

Complexes formed between metals and molecular oxygen have received extensive investigations, because they play important roles in fields of catalysis,[1,2] synthesis, materials, surface science,[3−6] and biochemistry.[7−10] The formation of $M(O_2)_n$ complexes (M = Cu, Ag, Au; n = 1, 2) have been investigated by infrared spectra in solid argon.[11] Kasai and Jones[12] reported ESR spectra of mono- and bis(dioxygen) complexes of Cu, Ag, and Au in solid argon and suggested ion pairs of the form $M^+(O_2)^-$, with $Cu(O_2)$ and $Ag(O_2)$ in bent end-on structures and $Au(O_2)$ in a symmetric side-on structure.[12] However, both $Ag(O_2)$ and $Au(O_2)$ were suggested to be side-on complexes from glassy matrix ESR spectra.[13] The $Pd(O_2)$ and $Pt(O_2)$ complexes appear to have the side-on structures based on matrix infrared isotopic spectra.[14,15]

Recently, laser-ablated transition-metal atom reactions with molecular oxygen have been studied extensively in this group. Various metal oxides, dioxides, superoxides, and peroxides as well as cations and anions have been identified from matrix infrared spectra.[15−25] However, most of the previous work has been done in a condensing argon matrix. In this paper, we report the reactions of laser-ablated Pd, Pt, Ag, and Au atoms with molecular oxygen in excess neon during condensation at 4 K because weakly bound complex products may be susceptible to different matrix interactions. Several neutral and negative metal−oxygen complexes are produced in the low-temperature matrix and identified by isotopic substitution and density functional theory (DFT) calculations.

Experimental Section

The experimental methods for reactions of laser-ablated metal atoms with small molecules during condensation in excess argon have been previously described in detail.[26,27] The Nd:YAG laser fundamental (1064 nm, 10 Hz repetition rate with 10 ns pulse width) was focused onto a rotating metal target. Gold and platinum (from crucibles), silver (99.9%), and palladium (99.9%) (Johnson-Matthey) metals were used as targets; the ablation laser energy was varied from 5 to 20 mJ/pulse. Laser-ablated metal atoms were co-deposited with molecular oxygen (0.2%−0.05%) in excess neon onto a 4 K CsI window at 1−2 mmol/h for 30 min. Oxygen (Matheson), isotopic $^{18}O_2$ (97.8% ^{18}O, Yeda), scrambled sample ($^{16}O_2/^{16}O^{18}O/^{18}O_2$ = 1:2:1), and mixed isotopic sample ($^{16}O_2/^{18}O_2$) were used in different experiments. Infrared spectra were recorded at 0.5 cm^{-1} resolution on a Nicolet 750 with 0.1 cm^{-1} accuracy using an HgCdTe detector. Matrix samples were annealed at different temperatures, and selected samples were subjected to broad-band photolysis by a medium-pressure mercury lamp (Philips, 175 W) with the globe removed.

Results

Infrared spectra of laser-ablated Pd, Pt, Ag, and Au atom reaction products with O_2 trapped in excess neon at 4 K are presented in Tables 1, 2 and Figures 1−8. Absorptions common in the experiments, namely O_3 (1039.9 cm^{-1}), O_4^- (972.9 cm^{-1}), *trans*-O_4^+ (1164.3 cm^{-1}), *cyclo*-O_4^+ (1320.2 cm^{-1}), and O_6^+ (1435.0 cm^{-1}), have been reported previously[25,28,29] and are not discussed here. Spectra after annealing and broad-band photolysis are also shown in the figures. Infrared spectra obtained using $^{18}O_2$ samples, mixed $^{16}O_2 + {}^{18}O_2$ samples, and scrambled $^{16}O_2 + {}^{16}O^{18}O + {}^{18}O_2$ samples are shown in Figures 2, 4, 6, and 8. In addition, several experiments were done with 0.02%−0.04% CCl_4 added to the 0.2% O_2 sample to serve as an electron trap, and the absorptions due to anions were eliminated from the spectra of the deposited samples.[30,31]

The density functional theoretical calculations of metal oxides and metal−oxygen complexes are given in Tables 3−8 for comparison. The Gaussian 94 program[32] was employed to calculate the structures and frequencies of expected metal−oxygen complexes, anions, and cations, using the BPW91 and B3LYP functionals.[33,34] The 6-311+G(d) basis set for oxygen and Los Alamos ECP plus DZ for metal atoms were used.[35,36] All the geometrical parameters were fully optimized, and the

* Corresponding author: lsa@virginia.edu.

10.1021/jp010058f CCC: $20.00
Published on Web 05/25/2001

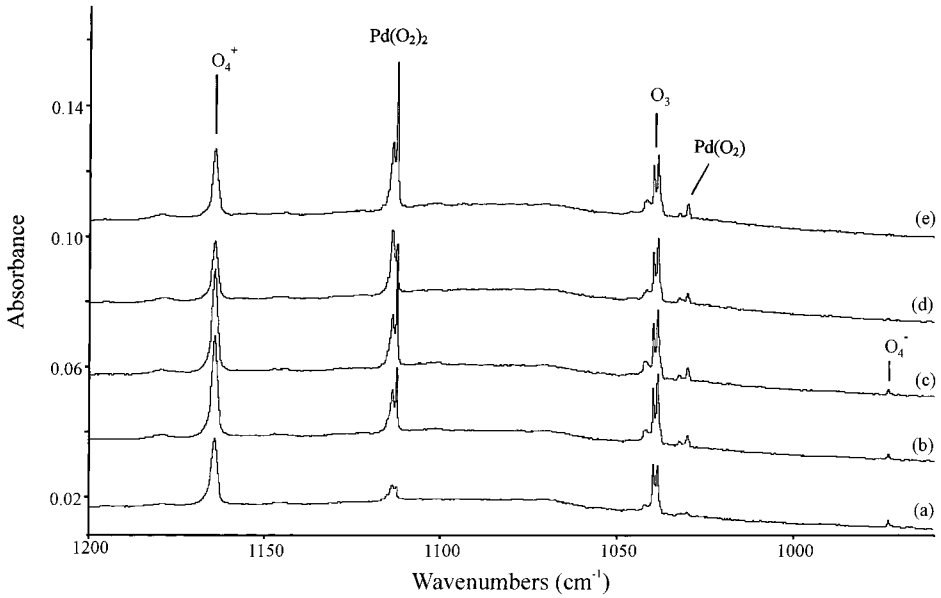

Figure 1. Infrared spectra in the 1200−950 cm^{-1} region for laser-ablated Pd atoms co-deposited with 0.1% O_2 in neon at 4−5 K. (a) Sample deposited for 60 min, (b) after annealing to 6 K, (c) after annealing to 8 K, (d) after full-arc photolysis for 20 min, and (e) after annealing to 10 K.

TABLE 1: Infrared Absorptions (cm^{-1}) from Co-deposition of Laser-Ablated Pd and Pt Atoms with O_2 in Excess Neon at 4 K

	$^{16}O_2$	$^{18}O_2$	$^{16}O_2 + {}^{16}O^{18}O + {}^{18}O_2$	$R(^{16}O/^{18}O)$	assignment
$Pd + O_2$	1113.7	1051.1			site
	1112.5	1050.0	1112.5, 1093.6, 1081.8, 1068.1, 1062.0, 1050.0	1.0595	Pd-(η^2−OO)$_2$
	1032.6				site
	1030.1	972.6	1030.2, 1001.9, 972.6	1.0591	Pd-(η^2−OO)
	973.0				
$Pt + O_2$	1057.1				site
	1056.0	997.0	1055.9, 1036.6, 1027.4, 1010.3, 1006.4, 997.0	1.0592	Pt-(η^2−OO)$_2$
	958.7	912.0	958.5, 944.2, 912.0, 867.7	1.0512	OPtO
	930.0	878.6	929.9, 904.8, 878.6	1.0585	Pt-(η^2−OO)
	839.7	793.9	839.7, 793.9	1.0577	PtO

TABLE 2: Infrared Absorptions (cm^{-1}) from Co-deposition of Laser-Ablated Ag and Au Atoms with O_2 in Excess Neon at 4 K

	$^{16}O_2$	$^{18}O_2$	$^{16}O_2 + {}^{18}O_2$	$^{16}O_2 + {}^{16}O^{18}O + {}^{18}O_2$	$R(^{16}O/^{18}O)$	assignment
$Ag + O_2$	2109.7	1995.2			1.0574	O_3
	2107.2	1992.1	2107.2, 2063.5, 2023.3, 1992.9		1.0578	O_3 (site)
	2074.9	1957.0	2073.9, 1957.0	2074.6, 2020.7, 2013.3, 1957.6	1.0603	$(Ag)_x$-(η^1-OO)
	2052.5	1936.4	2052.4, 1936.5	2052.8, 1999.8, 1991.6, 1936.7	1.0599	Ag-(η^1-OO)$^-$
	1102.5	1040.8		1102.4, 1076.9, 1069.6, 1040.8	1.0593	Ag-(η^1-OO)
	1042.1	983.6	1041.9, 984.0	1942.0, 1015.3, 1010.5, 982.6	1.0595	$(Ag)_x$-(η^1-OO)
	1030.7	972.9	1030.8, 972.9	1037.7, 1005.0, 999.9, 972.4	1.0594	Ag-(η^1-OO)$^-$
	1030.0	971.5	1030.0, 971.5	1029.8, 1004.2, 999.0, 971.5	1.0602	Ag-(η^1-OO)$^-$ (site)
	796.1	752.1	796.0, 786.5, 762.5, 752.1	796.1, 786.7, 776.3, 771.8, 762.5, 751.8	1.0585	$Ag^+O_3^-$
$Au + O_2$	1213.6	1144.8	1213.8, 1144.7	1212.9, 1180.3, 1144.4	1.0601	Au-(η^1-OO)
	1205.6	1138.3	1205.2, 1140.0		1.0591	Au-(η^1-OO) (site)
	911.9	861.2	911.9, 886.2, 863.0		1.0589	Au-(η^1-OO)$_2^-$
	824.2	784.2	824.2, 808.4, 784.2	824.1, 808.4, 784.0	1.0510	OAuO

harmonic vibrational frequencies were obtained analytically at the optimized structures. The computed geometric parameters, relative energies, dipole moments, frequencies, intensities, and isotopic frequency ratios are summarized in Tables 3−8. We find the lowest open OPdO structure to be a bent triplet state using the 6-311+G(d) basis set, in contrast to earlier calculations with the smaller D95* basis,[15] and to be higher in energy than the $Pd(O_2)$ complex. Platinum is different: OPtO is a linear singlet state and is more stable than the $Pt(O_2)$ complex. The Pd insertion into O_2 is sufficiently endothermic (calculated +27.0 kcal/mol) to prevent this reaction, but in contrast, the exothermic (calculated −56.4 kcal/mol) reaction to form OPtO is observed here.

Discussion

The new absorptions will be identified from isotopic shifts, splittings, and DFT frequency calculations.

Pd-(η^2-OO). The absorption at 1030.1 cm^{-1} in $Pd + O_2$/Ne experiments appeared on deposition, increased on annealing to 6 and 8 K, decreased on photolysis, and increased further on annealing to 10 K. This band shifted to 972.6 cm^{-1} in the $^{18}O_2$ experiments and gave the 1.0591 $^{18}O/^{16}O$ isotopic ratio. The scrambled $^{16}O_2 + {}^{16}O^{18}O + {}^{18}O_2$ sample gave triplets with 1:2:1 intensity profile at 1030.2, 1001.9, and 972.6 cm^{-1} indicating that two equivalent O atoms are involved in this vibration. The band at 1030.1 cm^{-1} can be assigned to the Pd-(η^2-OO) complex. (To simplify notation, the band is labeled $Pd(O_2)$ in

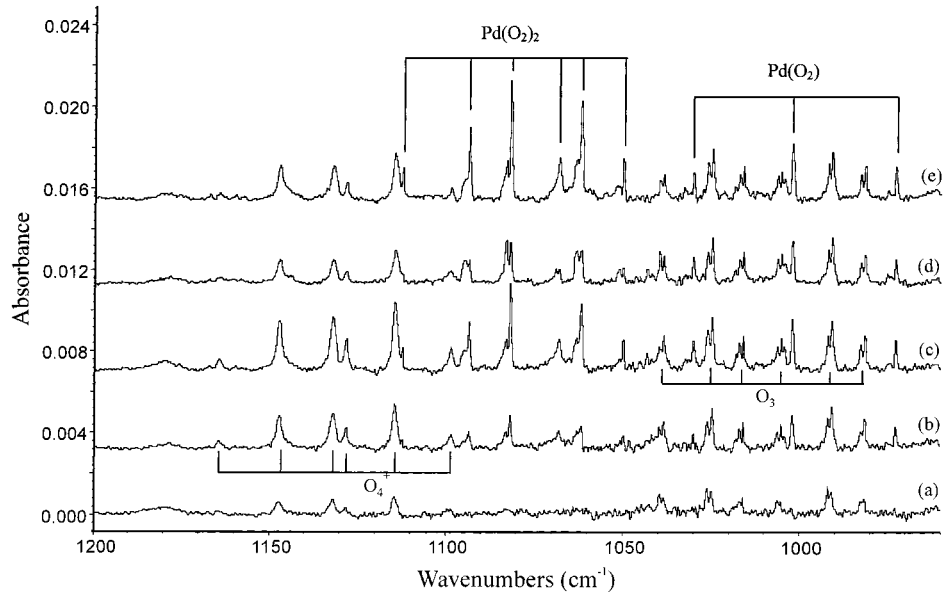

Figure 2. Infrared spectra in the 1200−950 cm^{-1} region for laser-ablated Pd atoms co-deposited with 0.05% ($^{16}O_2 + {}^{16}O^{18}O + {}^{18}O_2$) in neon. (a) Sample deposited for 60 min, (b) after annealing to 6 K, (c) after annealing to 8 K, (d) after full-arc photolysis for 20 min, and (e) after annealing to 10 K.

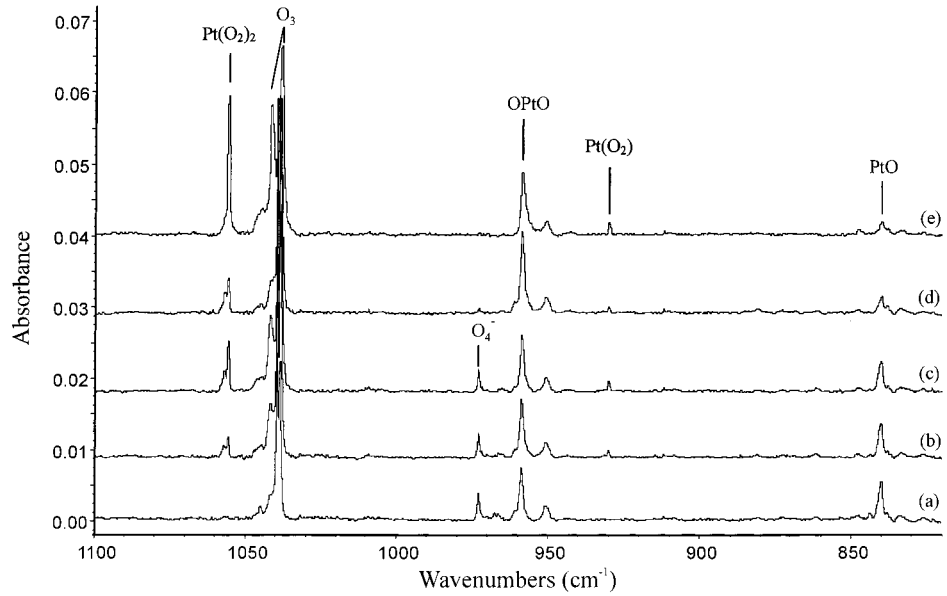

Figure 3. Infrared spectra in the 1100−820 cm^{-1} region for laser-ablated Pt atoms co-deposited with 0.1% O_2 in neon at 4−5 K. (a) Sample deposited for 60 min, (b) after annealing to 6 K, (c) after annealing to 8 K, (d) after full-arc photolysis for 20 min, and (e) after annealing to 10 K.

Figure 1.) This band was also observed at 1023.4 cm^{-1} in our previous argon matrix experiments[15] and in the early work of Huber et al.,[14] which identified a side-bonded $Pd(O_2)$ complex.

DFT calculations further support this assignment. The calculations (Tables 3 and 4) show that the Pd-(η^2-OO) complex has C_{2v} symmetry with a $^1A_1$ ground state. The O−O bond lengths are predicted to be 1.348 Å (BPW91) and 1.320 Å (B3LYP), which are much longer than that of free O_2. The calculated O−O stretching frequency at the BPW91 level is 1077.1 cm^{-1} with 1.0606 $^{16}O/^{18}O$ isotopic ratio, which is close to the observed neon matrix values (1030.1 cm^{-1}, $^{16}O/^{18}O$ = 1.0591). The calculated isotopic ratio for this mode at the B3LYP level is the same, but the predicted frequency (1160.3 cm^{-1}) is substantially higher, even higher than expected.[37] Scale factors (observed/calculated) are 0.956 (BPW91) and 0.853 (B3LYP). Clearly, this metal−molecular oxygen complex is modeled better by the BPW91 functional.

Pd-(η^2-OO)$_2$. The sharp band at 1112.5 cm^{-1} and matrix site at 1113.7 cm^{-1} are assigned to Pd-(η^2-OO)$_2$. This band was observed after deposition, increased greatly on annealing to 6 and 8 K, but decreased on broad-band photolysis. The $^{18}O_2$ counterpart for the 1112.5 cm^{-1} band appeared at 1050.0 cm^{-1}, giving the $^{16}O/^{18}O$ isotopic ratio 1.0595, which is very close to the value 1.0592 for Pd-(η^2-OO) and the 1110.1/1047.6 = 1.0596 ratio for the argon matrix counterparts.[20] The sextets observed in scrambled $^{16}O_2 + {}^{16}O^{18}O + {}^{18}O_2$ isotopic spectra (Figure 2) identify two equivalent OO subunits with equivalent atoms involved in an O−O stretching mode with side-bonded O_2, as found in early argon matrix work.[14]

Similar DFT calculations were done for Pd-(η^2-OO)$_2$, and results are listed in Tables 3 and 4. The predicted O−O bond lengths for the D_{2h} structure are 1.312 Å (BPW91) and 1.298 Å (B3LYP), which are slightly shorter than that in Pd-(η^2-OO), indicating the O−O bond is more reduced in Pd-(η^2-OO) than

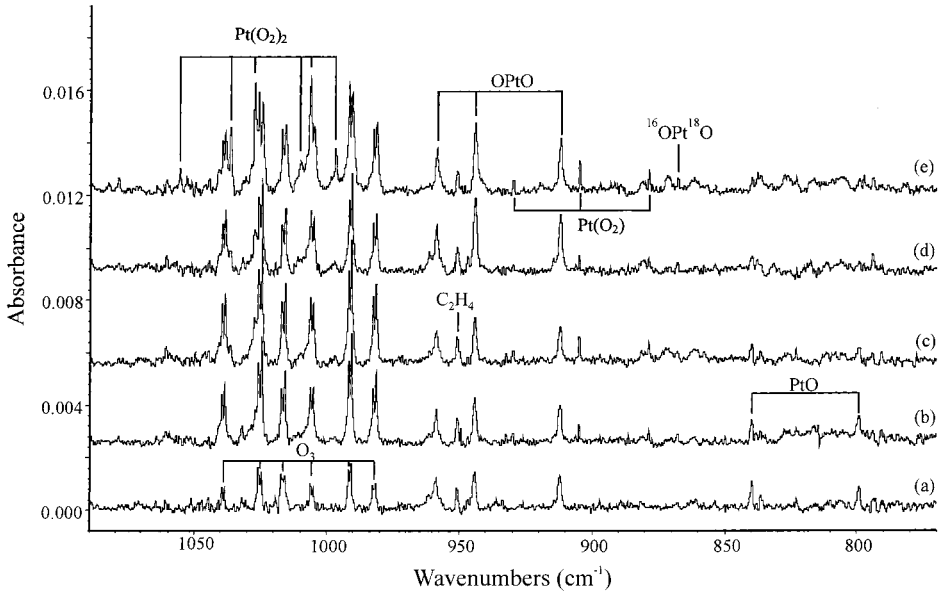

Figure 4. Infrared spectra in the 1090−770 cm^{-1} region for laser-ablated Pt atoms co-deposited with 0.1% O_2 in neon at 4−5 K. (a) Sample deposited for 60 min, (b) after annealing to 6 K, (c) after annealing to 8 K, (d) after full-arc photolysis for 20 min, and (e) after annealing to 10 K.

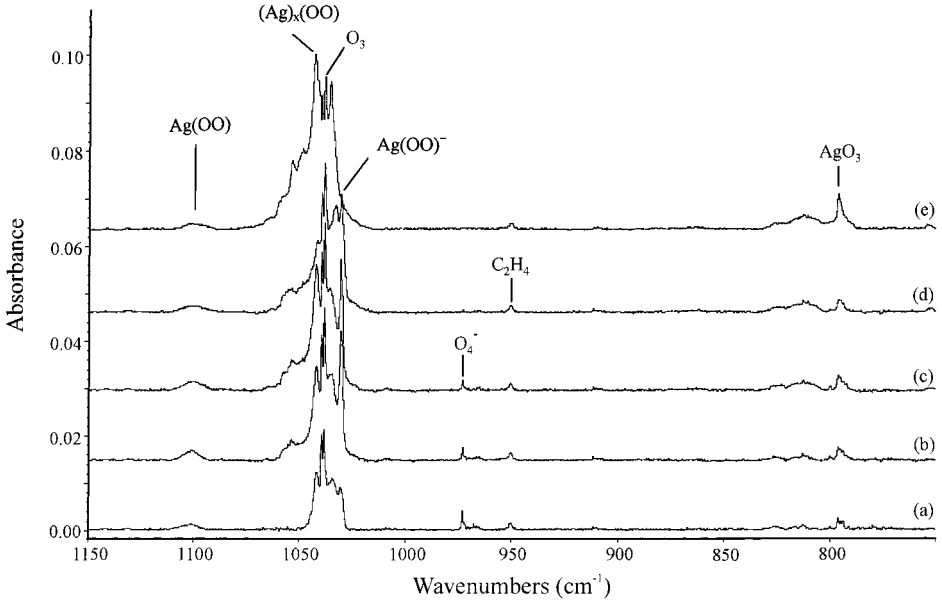

Figure 5. Infrared spectra in the 1150−750 cm^{-1} region for laser-ablated Ag atoms co-deposited with 0.2% O_2 in neon at 4−5 K. (a) Sample deposited for 60 min, (b) after annealing to 6 K, (c) after annealing to 8 K, (d) after full-arc photolysis for 20 min, and (e) after annealing to 10 K.

in Pd-(η^2-OO)$_2$. The calculated frequency of the O−O stretching mode at the BPW91 level is 1107.9 cm^{-1}, only 4.6 cm^{-1} lower than the 1112.5 cm^{-1} experimental value, and at the B3LYP level is 1145.6 cm^{-1}, only 33.1 cm^{-1} higher than the experimental value. The predicted $^{16}O/^{18}O$ isotopic ratios at both levels reproduce the experimental value very well.

The Pd-(η^2-OO)$_2$ structure with D_{2d} symmetry calculated at the B3LYP level is 2.2 kcal/mol higher in energy than the D_{2h} structure. The predicted frequency of the O−O stretching mode is 1194.4 cm^{-1}, which is 81.9 cm^{-1} higher than the experimental value. However, another important feature of the D_{2d} structure is the small imaginary 140.7 cm^{-1} frequency due to the degenerate (e symmetry) torsional mode around the C_2 axis, indicating that the D_{2d} structure is a second-order saddle point. Hence, we believe that the Pd-(η^2-OO)$_2$ complex, like the Ni analogue,[17] has the D_{2h} structure rather than the D_{2d} geometry first deduced.[14]

PtO and PtO_2. A sharp band was observed at 839.7 cm^{-1} after initial deposition, which showed a slight decrease on early annealing and a considerable decrease on broad-band photolysis (Figure 3). The $^{18}O_2$ counterpart for this band at 793.9 cm^{-1} gave a 1.0577 $^{16}O/^{18}O$ isotopic ratio. In the scrambled isotopic experiment, a doublet was observed, indicating only one oxygen atom. This band is assigned to the PtO molecule. The observed neon matrix frequency is very close to the 841.1 cm^{-1} fundamental deduced from the emission spectrum[38,39] and the 828.0 cm^{-1} argon matrix value.[15] The observed frequency also agrees with DFT calculations at 844.8 cm^{-1} (BPW91) and 843.5 cm^{-1} (B3LYP). The $^3\Sigma^-$ ground state is found by both BPW91 and B3LYP functional calculations.

The neon matrix absorption at 958.7 cm^{-1} is assigned to the PtO_2 molecule, which is slightly higher than our argon matrix observation of this species at 953.3 cm^{-1}.[15] In the scrambled isotopic experiment, a triplet 1:2:1 profile at 958.5, 944.2, and

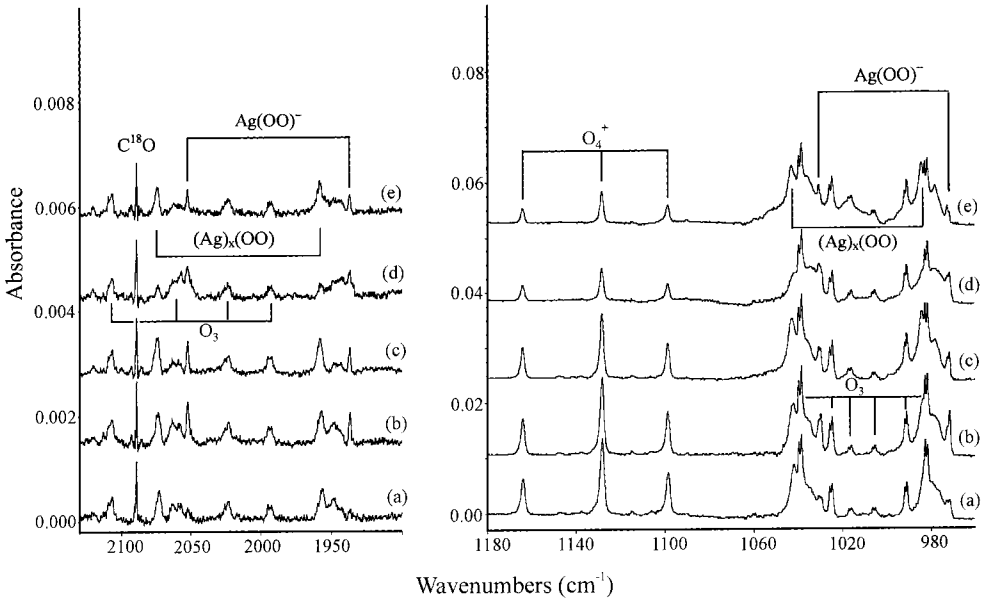

Figure 6. Infrared spectra in the 2130−1900 and 1180−960 cm^{-1} regions for laser-ablated Ag atoms co-deposited with 0.2% $^{16}O_2$ + 0.2% $^{18}O_2$ in neon at 4−5 K. (a) Sample deposited for 60 min, (b) after annealing to 6 K, (c) after annealing to 8 K, (d) after full-arc photolysis for 20 min, and (e) after annealing to 10 K.

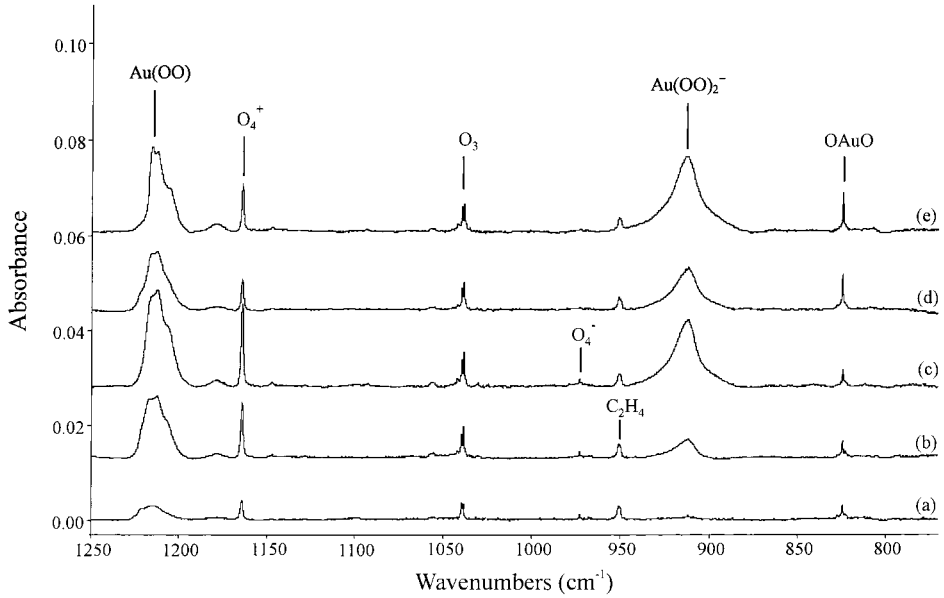

Figure 7. Infrared spectra in the 1250−750 cm^{-1} region for laser-ablated Au atoms co-deposited with 0.05% O_2 in excess neon at 4−5 K. (a) Sample deposited for 60 min, (b) after annealing to 6 K, (c) after annealing to 10 K, (d) after full-arc photolysis for 15 min, and (e) after annealing to 11 K.

912.0 cm^{-1} was observed, indicating that two equivalent oxygen atoms are involved in this molecule. The 1.0512 $^{16}O/^{18}O$ isotopic frequency ratio is much lower than the ratio observed for PtO and Pt-(η^2-OO), suggesting an antisymmetric O−Pt−O mode. In the scrambled isotopic experiment, a weak, new band at 867.7 cm^{-1} tracks with the 944.2 cm^{-1} band, and is due to the symmetric-stretching mode of $^{16}OPt^{18}O$. This observation agrees with our DFT calculations: both BPW91 and B3LYP functionals predict the PtO_2 molecule to have a $^1\Sigma_g^+$ ground state with the linear OPtO structure and an antisymmetric stretching mode at 962.2 cm^{-1} (BPW91) and 1013.6 cm^{-1} (B3LYP). Furthermore, the predicted separations of antisymmetric and symmetric modes of $^{16}OPt^{18}O$ are 69.5 cm^{-1} (BPW91) and 77.3 cm^{-1} (B3LYP), which agree with the experimental value (76.5 cm^{-1}). A bent triplet state is 25 kcal/mol higher in energy and has inappropriate frequencies.

Pt-(η^2-OO). The band at 930.0 cm^{-1} is assigned to the symmetric O−O stretching mode of Pt-(η^2-OO) in solid neon. This band shifts to 878.6 cm^{-1} in the $^{18}O_2$ experiment ($^{16}O/^{18}O$ isotopic ratio 1.0585). The 1:2:1 triplet in the scrambled isotopic experiment indicates that two equivalent oxygen atoms are involved. This observed frequency agrees with the 928.0 cm^{-1} argon matrix observation[14,15] and DFT calculations. The O−O stretching vibration was predicted at 966.6 cm^{-1} using the BPW91 functional, while a B3LYP calculation gave 1032.0 cm^{-1}, slightly higher than the BPW91 value. The calculated $^{16}O/^{18}O$ ratios, 1.0605 (BPW91) and 1.0605 (B3LYP), are slightly higher than the experimental ratio, 1.0585, owing to anharmonicity.

Pt-(η^2-OO)$_2$. The strong, sharp band at 1056.0 cm^{-1} is assigned to the O−O stretching frequency of Pt-(η^2-OO)$_2$, first observed at 1051 cm^{-1} in solid argon.[14,15] This band increased

TABLE 3: Relative Energies and Geometries Calculated at BPW91 and B3LYP Levels for MO_2, M-(η^2-OO), and M-(η^2-OO)$_2$ (M = Pd, Pt)

molecule	state	relative energy (kcal/mol)	μ^a	geometry (Å, degree)
		BPW91/6-311+G(d)/Lanl2DZ		
Pd-(η^2-OO)	$^1A_1$	0.0	4.47	PdO, 2.070; OO, 1.348; OPdO, 38.0
Pd-(η^2-OO)	$^3B_1$	+34.0	2.87	PdO, 2.255; OO, 1.261; OPdO, 32.5
OPdO	$^3A_2$	+9.7	2.39	PdO, 1.787; OPdO, 134.7
Pd-(η^2-OO)$_2$(D_{2h})	^1A_g	0.0	0.0	PdO, 2.067; OO, 1.312; OPdO, 37.0
Pt-(η^2-OO)	$^1A_1$	0.0	4.13	PtO, 2.005; OO, 1.403; OPtO, 41.0
OPtO	$^1\Sigma^+$	−58.1	0.0	PtO, 1.728; OPtO, 180.0
OPtO	$^3A_2$	−33.3	2.03	PtO, 1.776; OPtO, 135.2
Pt-(η^2-OO)$_2$(D_{2h})	^1A_g	0.0	0.0	PtO, 2.034; OO, 1.341; OPtO, 38.8
		B3LYP/6-311+G(d)/Lanl2DZ		
PdO	$^3\Sigma^-$		3.92	PdO, 1.863
Pd-(η^2-OO)	$^1A_1$	0.0	4.48	PdO, 2.072; OO, 1.320; OPdO, 37.1
OPdO	$^3A_2$	+27.8	2.88	PdO, 1.778; OPdO, 131.1
Pd-(η^2-OO)$_2$(D_{2h})	^1A_g	0.0	0.0	PdO, 2.043; OO, 1.298; OPdO, 37.1
Pd-(η^2-OO)$_2$(D_{2d})	$^1A_1$	+2.2	0.0	PdO, 2.062; OO, 1.313; OPdO, 37.1
PtO	$^3\Sigma^-$		3.03	PtO, 1.755
Pt-(η^2-OO)	$^1A_1$	0.0	4.45	PtO, 2.007; OO, 1.375; OPtO, 40.1
OPtO	$^1\Sigma^+$	−40.6	0.0	PtO, 1.714; OPtO, 180.0
OPtO	$^3A_2$	−20.7	2.31	PtO, 1.769; OPtO, 134.6
Pt-(η^2-OO)$_2$(D_{2h})	^1A_g	0.0	0.0	PtO, 2.011; OO, 1.328; OPtO, 38.6
Pt-(η^2-OO)$_2$(D_{2d})	$^1A_1$	+2.9	0.0	PtO, 2.001; OO, 1.367; OPtO, 40.0

[a] Dipole moment (Debye).

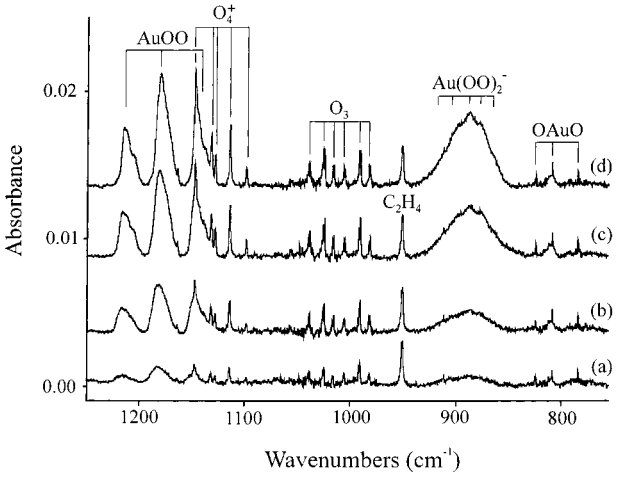

Figure 8. Infrared spectra in the 1250−750 cm^{-1} region for laser-ablated Au atoms co-deposited with 0.05% $^{16}O_2$ + $^{16}O^{18}O$ + $^{18}O_2$ in excess neon at 4−5 K. (a) Sample deposited for 60 min, (b) after annealing to 6 K, (c) after annealing to 10 K, and (d) after annealing to 10 K.

on annealing to 6 and 8 K, decreased on photolysis, and increased greatly on further annealing to 11 K. The $^{18}O_2$ counterpart for this band at 997.0 cm^{-1} gives a $^{16}O/^{18}O$ isotopic ratio of 1.0592, which is slightly higher than the ratio for Pt-(η^2-OO) and appropriate for the antisymmetric O−O stretching mode in the Pt-(η^2-OO)$_2$ molecule. The sextet in the $^{16}O_2$ + $^{16}O^{18}O$ + $^{18}O_2$ experiment suggests that two equivalent OO subunits are involved in this molecule. This assignment is confirmed by DFT calculations: both BPW91 and B3LYP functionals predicted that Pt-(η^2-OO)$_2$ has the ^1A_g ground state. The O−O stretching frequency was predicted at 1034.2 cm^{-1} at the BPW91 level, while the B3LYP functional gave 1064.8 cm^{-1}, which is slightly higher than the BPW91 value but very close to the experimental determination at 1056.0 cm^{-1}. The D_{2d} structure of Pt-(η^2-OO)$_2$ is 2.9 kcal/mol higher in energy than the D_{2h} structure calculated at the B3LYP level. Although the predicted frequency of the O−O stretching mode at 1084.0 cm^{-1} is close to the experimental observation, two equivalent, small negative frequencies at −51.7 cm^{-1} indicate a second-order saddle point. Similar conclusions have been reached for Ni-(η^2-OO)$_2$.[17] Our calculations disagree with the original proposal of D_{2d} structures[14] for these M(O$_2$)$_2$ molecules and provide strong evidence that the structures are D_{2h}.

TABLE 4: Bond-Stretching Isotopic Frequencies (cm^{-1}), Intensities (km/mol), and Frequency Ratios Calculated at the BPW91 and B3LYP Levels for the Structures Described in Table 3

molecule	state	^{16}O	^{18}O	$R(^{16}O/^{18}O)$
		BPW91/6-311+G(d)/Lanl2DZ		
PdO	$^3\Sigma^-$	621.9(13.7)	591.0(12.4)	1.0523
Pd-(η^2-OO)	$^1A_1$	1077.1(40)	1015.6(36)	1.0606
Pd-(η^2-OO)	$^3B_1$	1339.4(228)	1262.7(202)	1.0607
OPdO	$^3A_2$	771.6(54)	735.1(49)	1.4965
Pd-(η^2-OO)$_2$(D_{2h})	^1A_g	1107.9(551)	1044.6(490)	1.0606
Pt-(η^2-OO)	$^1A_1$	966.6(9)	911.5(8)	1.0605
PtO	$^3\Sigma^-$	844.8(28)	800.2((22)	1.0557
OPtO	$^1\Sigma^+$	962.2(115)	915.0(104)	1.0516
OPtO	$^3A_2$	797.3(45)	757.4(40)	1.0527
Pt-(η^2-OO)$_2$(D_{2h})	^1A_g	1034.2(408)	975.2(362)	1.0605
		B3LYP/6-311+G(d)/Lanl2DZ		
PdO	$^3\Sigma^-$	598.7(3.7)	569.0(3.4)	1.0522
Pd-(η^2-OO)	$^1A_1$	1160.3(77)	1094.0(68)	1.0606
Pd-(η^2-OO)$_2$(D_{2h})	^1A_g	1145.6(832)	1080.2(738)	1.0605
Pd-(η^2-OO)$_2$(D_{2d})	$^1A_1$	1194.4(149)	1126.5(131)	1.0603
Pt-(η^2-OO)	$^1A_1$	1032.0(26)	973.1(24)	1.0605
PtO	$^3\Sigma^-$	843.5(33)	798.9(30)	1.0558
OPtO	$^1\Sigma^+$	1013.6(150)	963.9(136)	1.0516
OPtO	$^3A_2$	797.3(36)	757.7(33)	1.0528
Pt-(η^2-OO)$_2$(D_{2h})	^1A_g	1064.8(625)	1004.2(555)	1.0604
Pt-(η^2-OO)$_2$(D_{2d})	$^1A_1$	1084.0(70)	1022.3(62)	1.0604

Ag-(η^1-OO). The thermal Ag experiments produced a 1078.9 cm^{-1} argon matrix band, which was assigned to Ag(O$_2$),[11c] and our laser-ablation investigation gave this band at 1075.7 cm^{-1} with an associated overtone at 2133.2 cm^{-1}.[24] However, with $^{16}O_2$ + $^{16}O^{18}O$ + $^{18}O_2$, both of these features give quartet patterns (2133.2, 2076.1, 2073.1, 2014.6 cm^{-1} and 1075.7, 1046.6, 1045.1, 1015.2 cm^{-1}), which suggest two inequivalent oxygen atoms.

A weak, broad 1102.5 cm^{-1} band appeared in neon matrix experiments on deposition, increased slightly on annealing, and decreased slightly on photolysis (Figure 5). This band shifted

TABLE 5: States, Relative Energies (kcal/mol), and Geometries Calculated at BPW91 and B3LYP Levels for Silver Oxygen Complexes and Oxides

molecule	state	rel energy	μ^a	geometry (Å, deg)
		BPW91/6-311+G(d)/Lanl2DZ		
Ag-(η^1-OO)[b]	$^2A''$	0.0	2.83	AgO, 2.311; OO, 1.266; AgOO, 118.8
	$^4A''$	7.6	0.04	AgO, 4.359; OO, 1.221; AgOO, 122.4
	$^2A'$	21.6	5.56	AgO, 2.158; OO, 1.314; AgOO, 115.9
Ag-(η^1-OO)$^-$	$^3A''$	−34.6	1.59	AgO, 2.640; OO, 1.295; AgOO, 123.0
	$^1A'$	−24.1	3.99	AgO, 2.251; OO, 1.339; AgOO, 120.3
	$^5A''$	−22.8	5.56	AgO, 4.311; OO, 1.221; AgOO, 115.2
Ag-(η^1-OO)$^+$	$^3A'$	180.2	1.98	AgO, 2.469; OO, 1.218; AgOO, 130.6
OAgO	$^4B_1$	52.4	0.0	AgO, 2.032; OAgO, 180.0
Ag-(η^1-OO)$_2$ (C_{2v})	$^4A_1$	0.0	0.80	AgO, 2.257; OO, 1.264; AgOO, 120.3; OAgO, 179.7
	$^2A_1$	9.4	0.87	AgO, 2.243; OO, 1.267; AgOO, 120.2; OAgO, 179.8
Ag-(η^1-OO)$_2^-$ (C_{2v})	$^3B_2$	−53.6	1.93	AgO, 2.189; OO, 1.333; AgOO, 114.9; OAgO, 178.1
$Ag^+O_3^-$	$^2B_2$		5.31	AgO, 2.329; OO, 1.361; OOO, 113.7; OAgO, 58.6
		B3LYP/6-311+G(d)/Lanl2DZ		
Ag-(η^1-OO)[c]	$^2A''$	0.0	2.61	AgO, 2.369; OO, 1.245; AgOO, 119.3
	$^4A''$	3.9	0.07	AgO, 3.894; OO, 1.206; AgOO, 122.0
	$^2A'$	19.4	6.60	AgO, 2.136; OO, 1.321; AgOO, 114.0
Ag-(η^1-OO)$^-$	$^3A''$	−36.8	2.16	AgO, 2.499; OO, 1.293; AgOO, 120.3
	$^1A'$	−20.9	4.13	AgO, 2.268; OO, 1.321; AgOO, 120.2
Ag-(η^1-OO)$^+$	$^3A''$	176.2	5.02	AgO, 2.469; OO, 1.204; AgOO, 136.1
OAgO	$^4\Sigma_g^+$	82.6	0.0	AgO, 1.916; OAgO, 180.0
Ag-(η^1-OO)$_2$ (C_{2v})	$^4B_1$	0.0	1.03	AgO, 2.168; OO, 1.268; AgOO, 121.1; OAgO, 178.8
	$^2B_2$	4.6	1.35	AgO, 2.174; OO,1.271; AgOO, 111.9; OAgO, 180.0
Ag-(η^1-OO)$_2^-$ (C_{2v})	$^3A_2$	−40.5	2.73	AgO, 2.099; OO, 1.345; AgOO, 111.5; OAgO, 177.8
$Ag^+O_3^-$	$^2B_1$		5.84	AgO, 2.325; OO, 1.343; OOO, 113.4; OAgO, 57.7

[a] Dipole moment (Debye). [b] The geometry of AgOO with BPW91 and SCI-PCM model (neon $\epsilon = 1.24$) AgO, 2.229; OO, 1.310, AgOO, 118.6°. [c] The geometry of AgOO with B3LYP and SCI-PCM model (neon $\epsilon = 1.24$) AgO, 2.203; OO, 1.543; AgOO, 111.1°.

TABLE 6: Bond-Stretching Isotopic Frequencies (cm^{-1}), Intensities (km/mol), and Frequency Ratios Calculated at BPW91 and B3LYP Levels for the Structures Described in Table 5

molecule	state	^{16}O	^{18}O	R ($^{16}O/^{18}O$)
		BPW91/6-311+G(d)/Lanl2DZ		
OAgO	$^4\Sigma_g^+$	449.3(0.3)	429.7(0.3)	1.0456
Ag-(η^1-OO)[a]	$^2A''$	1267.3(668)	1194.6(594)	1.0609
	$^4A''$	1540.7(0.1)	1452.4(0.1)	1.0608
	$^2A'$	1092.4(456)	1029.8(405)	1.0608
Ag-(η^1-OO)$^-$	$^3A''$	1174.3(877)	1107.0(779)	1.0608
	$^1A'$	1054.6(633)	994.2(562)	1.0608
	$^5A''$	1534.8(0.9)	1446.8(0.8)	1.0608
Ag-(η^1-OO)$^+$	$^3A'$	1515.9(15)	1429.1(13)	1.0607
	$^1A''$	1503.1(174)	1416.9(154)	1.0608
Ag-(η^1-OO)$_2$(C_{2v})	$^4A_1$	1263.3(1426)	1190.9(1268)	1.0608
	$^2A_1$	1251.8(1444)	1180.1(1332)	1.0608
Ag-(η^1-OO)$_2^-$(C_{2v})	$^3B_2$	1106.9(273)	1043.4(243)	1.0609
$Ag^+O_3^-$(C_{2v})	$^2B_2$	780.5(226)	735.8(201)	1.0608
		B3LYP/6-311+G(d)/Lanl2DZ		
OAgO	$^4\Sigma_g^+$	641.7(0.2)	613.6(0.2)	1.0458
Ag-(η^1-OO)[b]	$^2A''$	1325.2(1323)	1249.3(1175)	1.0608
	$^4A''$	1631.7(0.1)	1538.2(0.1)	1.0608
	$^2A'$	1078.8(391)	1017.0(347)	1.0607
Ag-(η^1-OO)$^-$	$^3A''$	1159.1(1355)	1092.6(1203)	1.0609
	$^1A'$	1096.5(1011)	1033.7(899)	1.0608
Ag-(η^1-OO)$^+$	$^3A''$	1621.7(5)	1528.8(5)	1.0608
Ag-(η^1-OO)$_2$(C_{2v})	$^4B_1$	1163.8(3652)	1097.1(3245)	1.0608
	$^2B_2$	1114.5(5691)	1050.7(5053)	1.0607
Ag-(η^1-OO)$_2^-$(C_{2v})	$^3A_2$	1122.0(34)	1057.7(30)	1.0608
$Ag^+O_3^-$(C_{2v})	$^2B_1$	861.6(329)	812.3(293)	1.0607

[a] The calculated O−O frequency with BPW91 and SCI−PCM Model (neon $\epsilon = 1.24$) 1100.5 cm^{-1} (1321.6 km/mol). Calculation failed to converge using argon. [b] The calculated O−O vibration with B3LYP and SCI−PCM Model (neon $\epsilon = 1.24$) 1153.2 cm^{-1} (5.2). Calculation failed to converge using argon.

to 1040.8 cm^{-1} with $^{18}O_2$ and gave a 1.0593 $^{16}O/^{18}O$ ratio, suggesting an O−O stretching vibration. The $^{16}O_2 + {}^{16}O^{18}O + {}^{18}O_2$ sample gave a broad 1070 cm^{-1} intermediate feature. Accordingly, this band must be considered for the AgOO complex as it is the only new absorption at higher wavenumbers than the 1075.7 cm^{-1} argon matrix band. Although the symmetric stretching mode of ozone is expected in this region,[40] the broad 1102.5 cm^{-1} band is too strong for the ozone present. With Pt and Pd, a very weak, sharp 1103.5 cm^{-1} band is observed with about 25% of the ozone band intensity at 700.0 cm^{-1}. In our Ag experiments, the broad 1102.5 cm^{-1} band is, however, much stronger than the sharp 700.0 cm^{-1} ozone absorption, and most of this absorption is due to AgOO.

Two doublet electronic states, $^2A''$ and $^2A'$, were calculated for Ag-(η^1-OO), and the latter is about 20 kcal/mol higher.[41] The calculated O−O stretching frequencies of the $^2A'$ state are 1092.4 cm^{-1} (BPW91) and 1078.8 cm^{-1} (B3LYP), respectively, which are in excellent agreement with the 1102.5 cm^{-1} neon matrix observation. However, the calculated O−O vibrations of the $^2A''$ state are 1267.3 cm^{-1} (BPW91) and 1325.2 cm^{-1} (B3LYP), which are much higher than the experimental value, although $^2A''$ was predicted to be the ground state. Here, polarization-induced charge transfer must be considered. The self-consistent isodensity-polarized continuum model (SCI-PCM) in the Gaussian 98 program[42] was used to describe the Ag-(η^1-OO) complex isolated in the low-temperature neon matrix. At both BPW91 and B3LYP levels, only the A″ electronic state is located for Ag-(η^1-OO), and the calculated frequencies (1100.5 and 1153.2 cm^{-1}, Table 6) are very close to the experimental value. It is concluded that partial charge transfer occurs when the Ag-(η^1-OO) complex is trapped in a solid matrix. This result agrees with the matrix ESR spectrum, which characterized AgOO as ionic.[13]

Ag-(η^1-OO)$^-$. The 1030.7 cm^{-1} band and its site at 1030.0 cm^{-1}, observed on sample deposition in Ag + O_2/Ne experiments, increased slightly on annealing, but decreased on full arc photolysis. Additional annealing failed to reproduce these bands, and they were eliminated with 0.02% CCl_4 added to the sample, strongly suggesting an anion species.[21,29−31] With the 0.2% $^{18}O_2$/Ne sample, the two bands shifted to 972.9 and 971.5 cm^{-1}, giving $^{16}O/^{18}O$ ratios 1.0594 and 1.0602, which is the

TABLE 7: States, Relative Energies (kcal/mol), and Geometries Calculated at BPW91 and B3LYP Levels for Gold Oxygen Complexes and Oxides

molecule	state	rel energy	μ^a	geometry (Å, deg)
		BPW91/6-311+ G(d)/Lanl2DZ		
Au-(η^1-OO)	$^2A''$	0.0	1.23	AuO, 2.197; OO, 1.249; AuOO, 119.0
	$^4\Sigma$	6.8	0.04	AuO, 4.348; OO, 1.221; AuOO, 180.0
Au- (η^1-OO)$^-$	$^3A''$	−54.7	1.64	AuO, 2.945; OO, 1.263; AuOO, 134.9
	$^1A'$	−42.6	4.07	AuO, 2.220; OO, 1.320; AuOO, 118.9
	$^5A''$	22.6	2.81	AuO, 3.792; OO, 1.225; AuOO, 123.7
Au-(η^1-OO)$^+$	$^3A''$	212.5	0.45	AuO, 2.286; OO, 1.215; AuOO, 122.3
OAuO	$^2\Pi_g$	31.8	0.00	AuO, 1.813; OAuO, 180.0
OAuO$^-$	$^3\Sigma_g^-$	−63.0	0.0	AuO, 1.895; OAuO, 180.0
	$^1A_1$	−40.0	0.45	AuO, 1.893; OAuO, 172.0
Au-(η^1-OO)$_2$(C_{2v})	$^4A_1$	0.0	0.31	AuO, 2.181; OO, 1.255; AuOO, 119.3; OAuO, 178.5
	$^2A_1$	9.4	0.38	AuO, 2.165; OO, 1.257; AuOO, 119.4; OAuO, 178.8
Au-cyc(OO)$_2$(C_{2v})	$^2A_2$	19.8	3.26	AuO, 2.231; OO, 1.266; AuOO, 113.5; OAuO, 85.4
Au-(η^1-OO)$_2^-$(C_{2v})	$^1A_1$	−54.3		AuO, 2.053; OO, 1.330; AuOO, 119.1; OAuO, 176.2
		B3LYP/6-311+G (d)/Lanl2DZ		
Au-(η^1-OO)	$^2A''$	0.0	0.52	AuO, 2.469; OO, 1.220; AuOO, 119.7
	$^4\Sigma$	0.9	0.07	AuO, 3.815; OO, 1.206; AuOO, 180.0
Au-(η^1-OO)$^-$	$^3A''$	−55.7	1.37	AuO, 2.944; OO, 1.245; AuOO, 123.4
	$^1A'$	−39.6	3.90	AuO, 2.225; OO, 1.304; AuOO, 118.6
OAuO	$^2\Pi_g$	50.8	0.0	AuO, 1.798; OAuO, 180.0
OAuO$^-$	$^3\Sigma_g^-$	−55.8	0.00	AuO, 1.881; OAuO, 180.0
	$^1A_1$	−30.7	0.66	AuO, 1.877; OAuO, 169.8
Au-(η^1-OO)$_2$	$^4A_1$	0.0	0.32	AuO, 2.232; OO, 1.235; AuOO, 119.6; OAuO, 179.2
	$^2B_1$	29.5	0.54	AuO, 2.041; OO, 1.262; AuOO, 119.3; OAuO,174.6
Au-(η^1-OO)$_2^-$	$^1A_1$	−72.7	1.84	AuO, 2.102; OO, 1.318; AuOO, 115.9; OAuO, 175.4

[a] Dipole moment (Debye).

TABLE 8: Bond-Stretching Isotopic Frequencies (cm^{-1}), Intensities (km/mol), and Frequency Ratios Calculated at BPW91 and B3LYP Levels for the Structures Described in Table 7

molecule	state	^{16}O	^{18}O	R (^{16}O/^{18}O)
		BPW91/6-311+G(d)/Lanl2DZ		
OAuO	$^2\Pi_g$	769.9(24)	732.1(21)	1.0517
OAuO$^-$	$^3\Sigma_g^-$	635.5(62)	604.3(55)	1.0517
	$^1A_1$	644.9(101)	613.2(89)	1.0517
Au-(η^1-OO)	$^2A''$	1316.5(437)	1241.0(389)	1.0608
	$^4\Sigma$	1541.9(0.1)	1453.5(0.1)	1.0608
Au- (η^1-OO)$^-$	$^3A''$	1295.2(770)	1220.9(684)	1.0609
	$^1A'$	1106.5(424)	1043.1(377)	1.0608
Au- (η^1-OO)$^+$	$^3A''$	1462.1(143)	1378.3(127)	1.0608
Au-(η^1-OO)$_2$(C_{2v})	$^4A_1$	1289.6(1020)	1215.6(906)	1.0609
	$^2A_1$	1275.2(1087)	1202.2(966)	1.0607
Au-cyc(OO)$_2$(C_{2v})	$^2A_2$	1170.3(561)	1103.2(498)	1.0608
		1268.8(128)	1196.1(114)	
Au-(η^1-OO)$_2^-$(C_{2v})	$^1A_1$	1051.3(912)	991.1(810)	1.0607
		B3LYP/6-311+G(d)/Lanl2 DZ		
OAuO	$^2\Pi_g^-$	800.8(23)	761.4(21)	1.0517
OAuO$^-$	$^3\Sigma_g^-$	675.9(53)	642.7(46)	1.0517
	$^1A_1$	690.0(103)	656.1(92)	1.0517
Au-(η^1-OO)	$^2A''$	1476.6(441)	1392.0(392)	1.0608
	$^4\Sigma$	1631.5(0.2)	1538.0(0.1)	1.0608
Au-(η^1-OO)$^-$	$^3A''$	1342.8(1541)	1265.8(1370)	1.0608
	$^1A'$	1150.9(673)	1084.9(578)	1.0608
Au-(η^1-OO)$_2$	$^4A_1$	1337.8(2424)	1261.1(2154)	1.0608
	$^2B_1$	1138.9(2890)	1073.6(2779)	1.0608
Au-(η^1-OO)$_2^-$	$^1A_1$	1057.1(1388)	996.6(1234)	1.0607

O−O stretching vibrational ratio. In the mixed $^{16}O_2 + {}^{18}O_2$ experiment, doublet bands at 1030.8 and 972.9 cm^{-1}, as well as 1030.0 and 971.5 cm^{-1}, were produced, which indicates that only one OO subunit is involved in this molecule. In addition, quartets with approximately 1:1:1:1 distributions were observed with the scrambled $^{16}O_2 + {}^{16}O^{18}O + {}^{18}O_2$ sample, suggesting one oxygen molecule coordinated to silver with the end-on structure.

The weak band centered at 2052.5 cm^{-1} has exactly the same behavior as the 1030.7 cm^{-1} absorption. This band appeared on deposition, increased on annealing, decreased on photolysis, and disappeared with CCl_4 added, suggesting different modes of the same molecule. The 1.0599 ^{16}O/^{18}O isotopic ratio of this band is very close to the ratio for the 1030.7 cm^{-1} band. Similar doublets with 1:1 shape in the mixed $^{16}O_2 + {}^{18}O_2$ experiment and quartets with 1:1:1:1 distribution in the $^{16}O_2 + {}^{16}O^{18}O + {}^{18}O_2$ experiment were also observed. This frequency is too high for an O−O stretching fundamental, so a combination or overtone band must be considered. The 2052.5 cm^{-1} band is 8.9 cm^{-1} less than 1030.7 × 2 = 2061.4 cm^{-1}, which is appropriate for anharmonicity and the overtone assignment.

The Ag-(η^1-OO)$^-$ anion assignment is further supported by theoretical calculations. Although the $^3A''$ state is calculated to be 12−16 kcal/mol lower than the $^1A'$ state, the O−O stretching frequencies 1054.6 cm^{-1} (BPW91, ^{16}O/^{18}O = 1.0608) and 1096.3 cm^{-1} (B3LYP, ^{16}O/^{18}O = 1.0609) calculated for the $^1A'$ state are in very good agreement with the observed 1030.7 cm^{-1} value (^{16}O/^{18}O isotopic ratio 1.0594), but the calculated $^3A''$ frequencies are 63−120 cm^{-1} higher. This suggests that $^1A'$ is actually the ground state.

$Ag^+O_3^-$. In the Ag + O_2/Ne experiment, a band observed after deposition at 796.1 cm^{-1} increased greatly on higher temperature annealing. This band shifted to 752.1 cm^{-1} with a 1.0585 ^{16}O/^{18}O isotopic ratio. Quartets in the mixed $^{16}O_2 + {}^{18}O_2$ experiment and sextets with the scrambled $^{16}O_2 + {}^{16}O^{18}O + {}^{18}O_2$ sample were observed, and the distributions of both quartets and sextets are analogues to isotopic spectra of the O_3 in the same sample. This band is assigned to the AgO_3 complex. A similar band was observed at 790 cm^{-1} in analogous argon matrix spectra[24] and at 791.8 cm^{-1} by Tevault et al.[43] The assignment is strongly supported by DFT calculations. The $\nu_3(O_3)$ mode frequency in the AgO_3 complex is predicted at 780.5 cm^{-1} with a 1.0608 ^{16}O/^{18}O isotopic ratio in BPW91 calculation, which agrees with the observed value, and a reasonable frequency at 861.6 cm^{-1} and a 1.0607 ratio is given by B3LYP calculation. The position of this frequency in the range of alkali metal ozonides[44] suggests a charge-transfer complex $Ag^+O_3^-$.

$(Ag)_x$-(η^1-OO). The absorption at 1042.1 cm^{-1} increased markedly on annealing, disappeared on photolysis, and re-

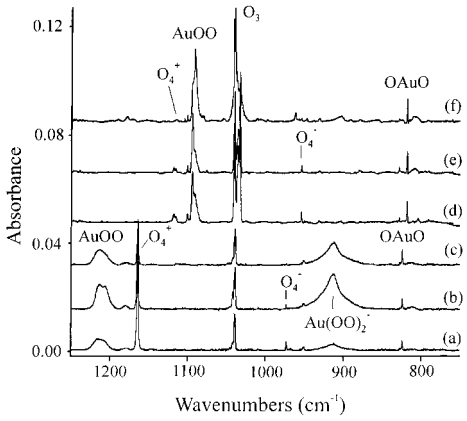

Figure 9. Infrared spectra in the 1250−750 cm^{-1} region for laser-ablated Au atoms co-deposited with 0.05% O_2 in excess noble gas. (a) 0.2% O_2 in neon co-deposited at 4−5 K, (b) after annealing to 8 K, (c) after full-arc photolysis, (d) 1% O_2 in argon co-deposited at 7−8 K, (e) after full-arc photolysis, and (f) after annealing to 40 K.

appeared on further annealing. In the experiments with CCl_4 added, the band was also observed, suggesting a neutral species. This band shifted to 983.6 cm^{-1} with $^{18}O_2$ and gave a 1.0595 $^{16}O/^{18}O$ ratio. The doublets with 1:1 relative intensities in mixed $^{16}O_2 + {}^{18}O_2$ experiments (Figure 6) and quartets with approximate 1:1:1:1 shape suggest a single O−O subunit analogous to the Ag-(η^1-OO) complex. The marked growth on annealing and appearance about 60 cm^{-1} lower suggests a higher complex, and $(Ag)_x$-(η^1-OO) is proposed for this band. The associated 2074.9 cm^{-1} band shifted to 1957.0 cm^{-1} with $^{18}O_2$ (1.0603 $^{16}O/^{18}O$ isotopic ratio), which is appropriate for O−O stretching vibrational ratios. This band tracked with the 1042.1 cm^{-1} band very well, and an overtone band of 1042.1 cm^{-1} must be considered; the 9.3 cm^{-1} difference between the observed 2074.9 cm^{-1} and 1042.1 × 2 = 2084.2 cm^{-1} is appropriate for anharmonicity.

Au-(η^1-OO). The broad band centered at 1213.6 cm^{-1} is assigned to the Au-(η^1-OO) complex. This band appeared on deposition, increased on annealing to 6 and 10 K, decreased on photolysis, and increased again on further annealing to 11 K (Figure 7). The 1213.6 cm^{-1} band shifts to 1144.8 cm^{-1} in the $^{18}O_2$ experiment with a 1.0601 $^{16}O_2/^{18}O_2$ isotopic ratio and shows the 1:1 doublet shape with mixed $^{16}O_2 + {}^{18}O_2$ sample. However, the scrambled $^{16}O_2 + {}^{16}O^{18}O + {}^{18}O_2$ sample gave a triplet centered at 1212.9, 1180.3, and 1144.4 cm^{-1}, suggesting that one OO subunit is involved in this molecule, but the attachment of OO to gold is uncertain because the broad isotopic bands cannot give structure information. However, our DFT calculations suggest that Au-(η^1-OO) has end-on coordination with a bent structure, which is analogous to the Ag-(η^1-OO) complex. The calculations predicted Au-(η^1-OO) to have a $^2A''$ ground state and O−O stretching vibration at 1316.5 cm^{-1} with a 1.0608 $^{16}O/^{18}O$ ratio (BPW91) and at 1476.6 cm^{-1} with a 1.0608 $^{16}O/^{18}O$ ratio (B3LYP), which are in excellent agreement with the observed isotopic ratio, but the frequency is overestimated by 100.8 cm^{-1} (BPW91) and 260.9 cm^{-1} (B3LYP).

Recall that a 1093.8/1091.7 cm^{-1} band has been assigned to AuO_2 in solid argon.[11c,24] The 1213.6 cm^{-1} neon matrix band appears to be counterpart to the 1093.8 cm^{-1} argon matrix band. This comparison (Figure 9) suggests that AuOO is substantially more ionic in the more polarizable argon matrix. A similar SCI-PCM calculation (BPW91) performed for $^2A''$ AuOO gave a 1310.7 cm^{-1} fundamental in neon and a 1302.8 cm^{-1} fundamental in argon ($\epsilon = 1.63$), which again shows the trend that the O−O stretching frequency decreases in the more polarizable matrix but does not account for the experimental differences. Although the more ionic $^2A'$ state for AuOO would not converge with DFT, a more ionic low-lying electronic state is suggested to be trapped in solid argon. Gold is capable of strong chemical bonds, and the weak Au−OO interaction will require still more sophisticated theoretical treatments.[45]

The mono(dioxygen) complexes of Cu, Ag, and Au have been studied by ESR spectroscopy. Howard et al.[13] reported that the two oxygen atoms in $Ag(O_2)$ and $Au(O_2)$ complexes are equivalent on the basis of the hyperfine structure from ^{17}O nuclei. However, a side-on structure of gold mono(dioxygen) complex was suggested in an analysis of the matrix isolation quadrupole interaction, although the ESR spectrum of $Au(O_2)$ was unusually complicated.[12] We conclude that two inequivalent oxygen atoms are involved in our neon matrix isolation spectra, and the end-on Au-(η^1-OO) structure is strongly suggested.

Au-(η^1-OO)$_2^-$. A broad band centered at 911.9 cm^{-1} exhibited sensitive annealing and photolysis behavior (Figure 8). This band appeared on annealing to 6 K, increased greatly on annealing to 10 K, but decreased on photolysis. The band shifted to 861.2 cm^{-1} with $^{18}O_2$ and gave a 1.0589 $^{16}O/^{18}O$ ratio, which characterizes an O−O stretching mode. Mixed $^{16}O_2 + {}^{18}O_2$ revealed an isotopic triplet, indicating the involvement of two OO subunits in this mode. Unfortunately, with the scrambled $^{16}O_2 + {}^{16}O^{18}O + {}^{18}O_2$ sample, the isotopic shape is not resolved due to the broad absorption. The 911.9 cm^{-1} band is eliminated by doping with CCl_4 in the sample to trap electrons during deposition, which strongly suggests an anion identification.[21,29−31] Assignment of this band to Au-(η^1-OO)$_2^-$ is supported by theoretical calculations. The $^1A_1$ ground state is predicted for Au-(η^1-OO)$_2^-$, and the O−O antisymmetric stretching frequency at 1051.3 cm^{-1} (BPW91) and 1057.1 cm^{-1} (B3LYP) are 13% higher than the observed 911.9 cm^{-1} band. The calculated $^{16}O/^{18}O$ isotopic ratio agrees with the experimental value. The symmetric vibrational mode was calculated to be much weaker and is not observed here.

AuO_2. The sharp band at 824.2 cm^{-1} is assigned to AuO_2, which was observed in argon matrix laser-ablation experiments at 817.9 cm^{-1}.[24] This reaction product was produced on sample deposition, increased 10% on annealing, and increased 100% on photolysis. The 1:2:1 triplet in the scrambled isotopic experiment (Figure 8) indicates two equivalent oxygen atoms in this molecule. The 824.2 cm^{-1} band exhibits a 1.0510 $^{16}O/^{18}O$ isotopic ratio, which is much lower than the ratio in molecular oxygen complexes and appropriate for a ν_3 fundamental in a linear O−Au−O molecule. The 824.2 cm^{-1} band appeared with about two-thirds of the absorbance in the CCl_4 doped experiment, so the anion identification is highly unlikely. Similarly, the 1% O_2 argon matrix experiment was repeated with 0.1% CCl_4, and the 817.9 cm^{-1} band was observed with 70% of the yield as in an identical control experiment without CCl_4. Our B3LYP functional calculation gave linear OAuO with an intense band at 800.8 cm^{-1} and a 1.0518 $^{16}O/^{18}O$ isotopic ratio, which matches the observed values very well. The BPW91 level calculation provided a reasonable frequency at 769.9 cm^{-1} and a 1.0516 $^{16}O/^{18}O$ isotopic ratio.[46] In contrast, the $OAuO^-$ anion calculations gave much lower frequencies (Table 8), which are not compatible with the observed spectrum.

Comparison of Metal−Oxygen Complexes and Matrices. The bonding of Pd, Pt, Ag, and Au atoms with molecular oxygen is quite different. In the Pd and Pt experiments, side-on M-(η^2-OO) (M = Pd, Pt) complexes are observed; however, end-on M-(η^1-OO) (M = Ag, Au) complexes are found in the Ag and

TABLE 9: Atomic Charge Distributions Based on Mulliken and Natural Bond Orbital Analysis (BPW91) and Observed O−O Stretching Frequencies for MO_2 Molecules

	charges						observed freq (cm^{-1})	
	Mulliken			natural bond orbital				
	metal	^1O	^2O	metal	^1O	^2O	neon	argon
Au-(η^1-OO) ($^2A''$)	0.064	−0.210	0.146	0.225	−0.154	−0.071	1213.6[a]	1093.8[c]
Ag-(η^1-OO) ($^2A''$)	0.278	−0.277	−0.001	0.340	−0.223	−0.117	1102.5[a]	1075.7[c]
Ag-(η^1-OO) ($^2A'$)	0.473	−0.378	−0.095	0.620	−0.418	−0.202	1102.5	1075.7
Pt-(η^2-OO) (C_{2v})	0.464	−0.232	−0.232	0.574	−0.287	−0.287[d]	930.0[a]	928.0[e]
Pd-(η^2-OO) (C_{2v})	0.404	−0.202	−0.202	0.488	−0.244	−0.244[f]	1030.1[a]	1023.0[e]
$Li^+(O_2^-)$	0.439	−0.220	−0.220	0.910	−0.455	−0.455	1093.8[b]	1096.9[g]

[a] This work. [b] Unpublished result in this group. [c] Reference 24. [d] Orbital breakdown: Pt[core] $6s^{0.46}$ $5d^{8.95}$ $6p^{0.10}$; O[core] $2s^{1.87}$ $2p^{4.39}$. [e] Reference 15. [f] Orbital breakdown: Pd[core] $5s^{0.19}$ $4d^{9.27}$; O[core] $2s^{1.86}$ $2p^{4.35}$. [g] Reference 49.

Au investigations. The Mulliken and natural bond orbital (NBO) charge distributions and experimental O−O stretching frequencies are listed in Table 9; the NBO distributions are expected to be more reliable.[47,48] The NBO charges on Pd and Pt in side-on M-(η^2-OO) are +0.57 and +0.49, but not near as high as for Li in the molecule $Li^+(O_2^-)$. The observed O−O stretching frequencies $Pd(O_2)$ and $Pt(O_2)$ are slightly lower than the O−O vibration in $Li^+(O_2^-)$, but the bonding mechanism is very different. The lithium superoxide molecule was first characterized as a highly ionic $Li^+(O_2^-)$ species,[49] and theoretical studies have verified the ionic model for the bonding.[50] Comparing the NBO electron configurations of $Pd(O_2)$ and $Pt(O_2)$, the 4d population of Pd is higher than the 5d population of Pt, but the 2p oxygen population in $Pd(O_2)$ is slightly lower than that in $Pt(O_2)$. These charges indicate that more back-donation from the Pt 5d to O_2 π^* occurs. Accordingly, the O−O bond is weakened in $Pt(O_2)$, and the insertion reaction can proceed with little barrier.

For end-on M-(η^1-OO) (M = Ag, Au) complexes, the Au atom is essentially neutral, and the charge on Ag is much higher, particularly in the $^2A'$ state. The O−O stretching frequency of Au-(η^1-OO) is much higher in solid neon than in solid argon, and the latter approaches the O−O vibration of $Li^+(O_2^-)$.

The neon−argon matrix host difference observed for these molecular oxygen complexes provides information about the guest species. The $Li^+(O_2^-)$, Pd-(η^2-OO), and Pt-(η^2-OO) species exhibit small differences (3, 7, and 2 cm^{-1}, respectively) between neon and argon matrixes (Table 9), which show that the bonding and O−O frequency are affected little by a change in the polarizability of the medium, which is typical for most molecules.[51] Note that the least ionic of these molecules $Pd(O_2)$ exhibits the largest difference. This is much more pronounced for Ag-(η^1-OO) and Au-(η^1-OO), where the O−O frequency is clearly medium-dependent. The Ag-(η^1-OO) and Au-(η^1-OO) complexes exhibit 27 and 120 cm^{-1} neon−argon differences, respectively, suggesting that these two complexes increase charge transfer in the more polarizable argon host. As a result, the O−O stretching frequencies observed in the argon matrix are very close to the same mode for $Li^+(O_2^-)$. In this regard, ESR spectra suggest that these complexes are highly ionic in solid argon, but AuOO was not examined in solid neon.[12] The difference between Ag and Au here is due in part to the greater relativistic effect (and inertness) for gold.[52]

Reaction Mechanisms. The metal dioxides, OPtO and OAuO, were observed in our experiments, but the relative yields are different. In the Pt + O_2 experiment, the OPtO molecule is a major product after sample deposition. It is concluded that the platinum atoms generated by laser ablation have sufficient excess energy to activate the O−O bond and give the OPtO insertion product. However, further annealing cannot increase PtO_2 but does produce the oxygen molecular complex Pt-(η^2-OO) (reaction 1). The B3LYP energy will be used to discuss the reaction mechanism because B3LYP calculations typically give more reliable energies.

$$Pt + O_2 \text{ annealing} \rightarrow Pt\text{-}(\eta^2\text{-OO}) \qquad \Delta E = -2.3 \text{ kcal/mol} \quad (1)$$

This reaction is exothermic by 2.3 kcal/mol. In addition, OPtO can be produced on broad-band photolysis at the expense of Pt-(η^2-OO):

$$Pt\text{-}(\eta^2\text{-OO}) + \text{photolysis} \rightarrow OPtO \qquad \Delta E = -40.6 \text{ kcal/mol} \quad (2)$$

Insertion reaction 2 is even more exothermic: this means that the rearrangement of the molecular complex is thermodynamically favorable but has an energy barrier. The behavior is analogous to the reactions of platinum and molecular oxygen in solid argon,[14,15] and recent thermal Pt reactions form OPtO only on photolysis.[53]

In the Au + O_2 experiments, a weak OAuO band at 824.2 cm^{-1} was observed following deposition. This indicates that gold atoms generated from laser ablation do not react with molecular oxygen as effectively as ablated platinum atoms, although ablated Au atoms also have excess translational and metastable electronic energy. The Au-(η^1-OO) complex is the major product formed on sample annealing, which is exothermic by 1.2 kcal/mol (reaction 3). However, the insertion reaction from Au-(η^1-OO) to OAuO is *endothermic* by 50.8 kcal/mol (reaction 4), but the reaction is observed on broad-band UV photolysis. The weak intermediate $^{16}OAu^{18}O$ band observed at 808.4 cm^{-1} with $^{16}O_2 + {}^{18}O_2$ suggests that some OAuO is made from O atom reaction 5. Although AuO was not observed in our neon matrix experiments, presumably due to reaction 5, AuO was found at 619.2 cm^{-1} in solid argon.[24]

$$Au + O_2 \text{ annealing} \rightarrow Au\text{-}(\eta^1\text{-OO}) \qquad \Delta E = -1.2 \text{ kcal/mol} \quad (3)$$

$$Au\text{-}(\eta^1\text{-OO}) \rightarrow AuO_2 \qquad \Delta E = +50.8 \text{ kcal/mol} \quad (4)$$

$$O + AuO \rightarrow OAuO \quad (5)$$

It is interesting to note that Ag-$(\eta^1$-OO$)^-$ was produced in Ag + O_2 experiments, but Au-$(\eta^1$-OO$)_2^-$ was observed in Au + O_2 experiments. Here, the electron affinity may play an important role in the formation of the anions. The ground-state Ag-$(\eta^1$-OO$)^-$ anion was calculated to be 36.8 kcal/mol lower in energy than the neutral Ag-(η^1-OO) complex, so the electron affinity of the neutral Ag-(η^1-OO) is estimated to be about 1.6 eV. The electron affinity of Ag-$(\eta^1$-OO$)_2$ is predicted to be 40.5 kcal/mol, which is close to the value of Ag-(η^1-OO). However, the Au-$(\eta^1$-OO$)_2^-$anion is calculated to be 72.7 kcal/mol lower than the neutral counterpart, indicating that the electron affinity of Au-$(\eta^1$-OO$)_2$ is much higher than that of Ag-$(\eta^1$-OO$)_2$. As expected, Ag-$(\eta^1$-OO$)^-$ and Au-$(\eta^1$-OO$)_2^-$ were observed in

the experiments. The Au-(η^1-OO)$_2^-$ anion band increased on annealing after photolysis, suggesting a very high electron affinity for Au(OO)$_2$. Although Au(OO)$_2$ was not observed here, Au(OO)$_2^-$ can be formed by reaction of Au(OO) and O_2^-; the latter is involved in the formation of O_4^-, which is observed in these experiments.[28,29]

Conclusions

Laser-ablated palladium, platinum, silver, and gold atoms react with molecular oxygen in excess neon during condensation at 4 K. Further reactions on annealing and photolysis are investigated. The reaction products were identified on the basis of the isotopic shifts of $^{18}O_2$ and isotopic multiplets for mixed $^{16}O_2 + {}^{18}O_2$ and scrambled $^{16}O_2 + {}^{16}O^{18}O + {}^{18}O_2$ samples. The side-on Pd-(η^2-OO) and Pd-(η^2-OO)$_2$ complexes were observed after sample deposition and further annealing, while similar complexes, Pt-(η^2-OO) and Pt-(η^2-OO)$_2$, were produced in the reaction of platinum atoms with molecular oxygen. The O−O stretching frequencies of M-(η^2-OO) (M = Pd, Pt) are lower than the O−O vibration in the Li$^+$(O_2^-) molecule, but the bonding mechanisms are different: d orbitals are involved, and Pt(O_2) exhibits the effect of more d orbital back-bonding than Pd(O_2). In addition, the insertion product OPtO was formed via the reaction of platinum atoms generated by laser ablation with molecular oxygen and by photoisomerism of PtO_2.

In the Ag, Au + O_2 experiments, end-on M-(η^1-OO) (M = Ag, Au) complexes were produced, which represent different bonding from side-on M-(η^2-OO) (M = Pd, Pt). The analogous OAuO dioxide molecule was observed. In addition, the anions Ag-(η^1-OO)$^-$ and Au-(η^1-OO)$_2^-$ were formed by electron-capture processes. Doping with CCl_4 to serve as an electron trap gave the same neutral molecules but eliminated the anion bands, which further supports the anion identifications.[21,29−30]

The good agreement with frequencies and isotopic frequency ratios from BPW91 and B3LYP density functional calculations further supports the vibrational assignments. The natural bond orbital charge distributions in M(O_2) molecules show increased charge transfer in the order Au < Pd < Pt < Ag (^{2}A′) < Li, and there is an unusual matrix effect for the least ionic (AuOO) of these.

The complexes M-(η^2-OO) (M = Pd, Pt) and molecular Li$^+$(O_2^-) show 3−7 cm^{-1} argon−neon blue shifts, but Ag-(η^1-OO) and Au-(η^1-OO) exhibit 27 and 120 cm^{-1} differences, respectively, suggesting that these two complexes undergo more charge transfer in the argon matrix. We attribute this difference to the stabilization of increased charge transfer by the more polarizable argon matrix.

Acknowledgment. We acknowledge support for this research from the National Science Foundation.

References and Notes

(1) Novvakova, J.; Brabec, L. *J. Catal.* **1997**, *166*, 186.
(2) Zambelli, T.; Barth, J. V.; Wintterlin, J. *Nature* **1997**, *390*, 495.
(3) Bao, X.; Muhler, M.; Schedelniedrig, T.; Schlogl, R. *Phys. Rev. B* **1996**, *54*, 2249.
(4) Zou, S. Z.; Chan, H. Y. H.; Williams, C. T.; Weaver, M. J. *Langmuir* **2000**, *16*, 754.
(5) Maya, L.; Paranthaman, M.; Thundat, T.; Bauer, M. L. *J. Vac. Sci. Technol., B* **1996**, *14*, 15.
(6) Wadayama, T.; Suzuki, O.; Suzuki, Y.; Hatta, A. *Appl. Phys. A* **1997**, *64*, 501.
(7) Andrews, L.; Chertihin, G. V.; Ricca, A.; Bauschlicher, C. W., Jr. *J. Am. Chem. Soc*. **1996**, *118*, 467.
(8) Potter, W. T.; Tucker, M. P.; Houtchens, R. A.; Caughey, W. S. *Biochemistry* **1987**, *26*, 4699.
(9) Hirota, S.; Ogura, T.; Appleman, E. H.; Shinzawa-Itah, K.; Yoshikawa, S.; Kitagawa, T. *J. Am. Chem. Soc*, **1994**, *116*, 10564.
(10) Hirota, S.; Ogura, T.; Kitagawa, T. *J. Am. Chem. Soc*. **1994**, *116*, 10564.
(11) (a) Tevault, D. E. *J. Chem. Phys.* **1982**, *76*, 2859. (b) Ozin, G. A.; Mitchell, S. A.; Garcia-Prieto, J. *J. Am. Chem. Soc.* **1983**, *105*, 6399; *J. Phys. Chem.* **1982**, *86*, 473. (c) McIntosh, D.; Ozin, G. A. *Inorg. Chem.* **1976**, *15*, 2869; **1977**, *16*, 59 (Ag, Au + O_2).
(12) Kasai, P. H.; Jones, P. M. *J. Phys. Chem*. **1986**, *90*, 4239.
(13) Howard, J. A.; Sutcliffe, R.; Mile, B. *J. Phys. Chem*. **1984**, *88*, 4351.
(14) Huber, H.; Klotzbucher, W.; Ozin, G. A.; Vander Voet, A. *Can J. Chem*. **1973**, *51*, 2722.
(15) Bare, W. D.; Citra, A.; Chertihin, G. V.; Andrews, L. *J. Phys. Chem. A* **1999**, *103*, 5456 (Pd, Pt + O_2 in argon).
(16) Chertihin, G. V.; Andrews, L. *J. Phys. Chem*. **1995**, *99*, 6356 (Ti, Zr, Hf + O_2 in argon).
(17) Citra, A.; Chertihin, G. V.; Andrews, L.; Neurock, M. *J. Phys. Chem. A* **1997**, *101*, 3109 (Ni + O_2 in argon).
(18) Chertihin, G. V.; Andrews, L.; Bauschlicher, C. W., Jr. *J. Phys. Chem. A* **1997**, *101*, 4026 (Cu + O_2 in argon).
(19) Zhou M. F.; Andrews, L. *J. Phys. Chem. A* **1998**, *102*, 8251 (Ta, Nb + O_2 in argon).
(20) Bare, W. D.; Souter, P. F.; Andrews, L. *J. Phys. Chem. A* **1998**, *102*, 8279. (Mo, W + O_2 in argon).
(21) Zhou, M. F.; Andrews, L. *J. Chem. Phys.* 1999, *111*, 4230 (Cr, Mo, W + O_2 in neon).
(22) Citra, A.; Andrews, L. *J. Phys. Chem. A* **1999**, *103*, 4182 (Ir + O_2 in argon).
(23) Citra, A.; Andrews, L. *J. Phys. Chem. A* **1999**, *103*, 4845 (Rh + O_2 in argon).
(24) Citra, A.; Andrews, L. *J. Mol. Struct.* **1999**, *189*, 95 and unpublished results (Ag, Au + O_2).
(25) Zhou, M. F.; Citra, A.; Liang, B.; Andrews, L. *J. Chem. Phys. A* **2000**, *104*, 3457 (Re, Ru, Os + O_2).
(26) Burkholder, T. R.; Andrews, L. *J. Chem. Phys*. **1991**, *95*, 8697.
(27) Hassanzadeh, P.; Andrews, L. *J. Phys. Chem*. **1992**, *96*, 9177.
(28) Thompson, W. E.; Jacox, M. E. *J. Chem. Phys*. **1989**, *91*, 3826.
(29) Zhou, M. F.; Hacaloglu, J.; Andrews, L. *J. Chem. Phys*. **1999**, *110*, 9450.
(30) Zhou, M. F.; Andrews, L. *J. Chem. Phys*. **1999**, *110*, 10370.
(31) Zhou, M. F.; Andrews, L. *J. Am. Chem. Soc*. **1998**, *120*, 11499.
(32) Frisch, M. J.; Trucks, G. W.; Schlegel, H. B.; Gill, P. M. W.; Johnson, B. G.; Robb, M. A.; Cheeseman, J. R.; Keith, T.; Petersson, G. A.; Montgomery, J. A.; Raghavachari, K.; Al-Laham, M. A.; Zakrzewski, V. G.; Ortiz, J. V.; Foresman, J. B.; Cioslowski, J.; Stefanov, B. B.; Nanayakkara, A.; Challacombe, M.; Peng, C. Y.; Ayala, P. Y.; Chen, W.; Wong, M. W.; Andres, J. L.; Replogle, E. S.; Gomperts, R.; Martin, R. L.; Fox, D. J.; Binkley, J. S.; Defrees, D. J.; Baker, J.; Stewart, J. P.; Head-Gordon, M.; Gonzalez, C.; Pople, J. A. *Gaussian 94*, revision B.1; Gaussian Inc.: Pittsburgh, PA, 1995.
(33) (a) Becke, A. D. *Phys. Rev. A* **1988**, *38*, 3098. (b) Perdew, J. P.; Wang, Y. *Phys. Rev. B* **1992**, *45*, 13244.
(34) (a) Becke, A. D. *J. Chem. Phys.* **1993**, *98*, 5648. (b) Lee, C.; Yang, W.; Parr, R. G. *Phys. Rev. B* **1988**, *37*, 785.
(35) (a) Krishnan, R.; Binkley, J. S.; Seeger, R.; Pople, J. A. *J. Chem. Phys.* **1980**, *72*, 650. (b) Frisch, M. J.; Pople, J. A.; Binkley, J. S. *J. Chem. Phys.* **1984**, *80*, 3265.
(36) (a) Wadt, W. R.; Hay, P. J. *J. Chem. Phys.* **1985**, *82*, 284. (b) Hay, P. J.; Wadt, W. R. *J. Chem. Phys.* **1985**, *82*, 299.
(37) Bytheway, I.; Wong, M. W. *Chem. Phys. Lett.* **1988**, *282*, 219.
(38) Nilsson, C.; Scullman, R.; Mehendale, N. *J. Mol. Spectrosc*. **1970**, *35*, 172. Scullman, R.; Sassenberg, U.; Nilsson, C. *Can. J. Phys*. **1975**, *53*, 1991. Jansson, K.; Scullman, R. *J. Mol. Spectrosc*. **1976**, *61*, 299. Sassenberg, U.; Scullman, R. *J. Mol. Spectrosc*. **1977**, *68*, 331.
(39) Srdanov, V. I.; Harris, D. O. *J. Chem. Phys*. **1987**, *89*, 2748.
(40) Andrews, L.; Spiker, R. C., Jr. *J. Phys. Chem.* **1972**, *76*, 3208.
(41) A BPW91/6-311+G**/SDD calculation produced the same result: the ^{2}A″ state is lower than ^{2}A′ by 21.6 kcal/mol.
(42) Foresman, J. B.; Keith, T. A.; Wiberg, K. B.; Snoonian, J.; Frisch, M. J. *J. Phys. Chem.* **1996**, *100*, 16098.
(43) Tevault, D. E.; DeMarco, R. A.; Smardzewski, R. R. *J. Chem. Phys.* **1981**, *75*, 4168.
(44) Spiker, R. C., Jr.; Andrews, L. *J. Chem. Phys.* **1973**, *59*, 1851.
(45) Barysz, M.; Pyykko, P. *Chem. Phys. Lett.* **1998**, *285*, 149.
(46) Calculations with a larger basis set gave slightly higher frequencies, see ref 24.
(47) Reed, A. J.; Curtiss, L. A.; Weinhold, F. *Chem. Rev.* **1988**, *88*, 899.
(48) Frenking, G.; Frohlich, N. *Chem. Rev.* **2000**, *100*, 717.
(49) Andrews, L. *J. Chem. Phys.* **1969**, *50*, 4288.
(50) Allen, W. D.; Horner, D. A.; Dekock, R. L.; Remington, R. B.; Schaefer, H. F., III. *Chem. Phys.* **1989**, *133*, 11 and references therein.
(51) Jacox, M. E. *Chem. Phys.* **1994**, *189*, 149.
(52) Pyykko, P. *Chem. Rev.* **1988**, *88*, 563.
(53) Manceron, L., to be published.